# INFLUENCE OF DARK COUNT ON THE PERFORMANCE OF SILICON PHOTOMULTIPLIERS

A. Intermite#, M. Putignano, C.P. Welsch, The Cockcroft Institute, Warrington WA4 4AD, UK,
Department of Physics, University of Liverpool, Liverpool L69 7ZE, UK

*Abstract*

The introduction of Silicon Photomultipliers (SiPMs) as single photon sensitive detectors represents a promising alternative to traditional photomultiplier tubes. This is especially true in applications in which it is compulsory to attain magnetic field insensitivity, low photon flux detection, quantum efficiency in the blue region that is comparable to standard photomultipliers, high timing resolution, dimensions comparable to the dimensions of an optical fiber diameters, and low costs. The structure of the SiPM is based on an array of independent Avalanche Photodiodes (APDs) working in Geiger-mode at a low bias voltage with a high gain. The output signal is proportional to the number of pixels "fired" by impacting photons. The detection efficiency for state-of-the-art devices is in the order of 20% at 500 nm. In this contribution, the measured dark count rates of different SiPMs are compared and the signal shape and statistical spectrum of this noise analyzed. A characterization of the effects on the noise of the bias voltage is performed as part of the study to determine the optimized working parameters for a future beam loss monitor at CTF3/CLIC.

## INTRODUCTION

Sensors capable of detecting single photons have found different applications in fields as astronomy [1] laser ranging [2], Optical Time Domain Reflectometry (OTDR) [3] and beam loss detection [4], replacing in such applications the former use of photomultiplier tubes (PMTs). The need to reduce the detector dimensions and to produce marketable nanotechnology applications require the use of small area, highly sensitive detectors that combine integrated readout circuitry functionality in a cheap fabrication process. In addition, small area detectors can be easily integrated in a dense array, be coupled with optical fibers, and reach high sensitivities.

Due to their high quantum efficiency, magnetic field immunity, robustness, low costs, possibility to operate at non-cryogenic temperatures and single photon detection capability, SiPMs are considered a suitable candidate for the readout of optical fibers in a beam loss detection system [4].

In this contribution, the operation principle of the beam loss monitor that will be used at CLEX/CLIC is introduced before a noise study for the SiPM, providing both a theoretical description and a set of experimental data, is described in detail. Within the analysis the behaviour of the noise with respect to the bias voltage applied to the SiPM by the user and to the quality of the manufacturing features dependent on the supplier are explored.

## BEAM LOSS DETECTION

For detecting and localizing beam losses in an accelerator, it is possible to exploit the generation of Cerenkov light inside optical fibers generated by impinging charged relativistic particles. At the locations where particles are lost from the main beam in the accelerator, these are likely to generate secondary particles through interaction with material, such as the beam pipe. These secondary charged particles are typically moving at relativistic velocities, hence, when they cross a medium with high enough dielectric constant, such as an optical fiber, they generate photons by the so-called *Cerenkov Effect* [5]. In such a configuration the fiber can be used to guide these photons to a SiPM, optically coupled to the fiber end [6]. In order to detect the beam losses at CTF3/CLIC, a system consisting of two parallel fibers connected to two identical SiPMs with an active surface matched to the fiber core of 1 $mm^2$ is under consideration.

The first fiber is used to carry a reference signal, and is chosen to be a low attenuation multimode fiber with a large core diameter. This maximizes the length of interaction with the escaping particles and thus the production of Cerenkov photons. The second arm is instead a composite sensor, realized by separating equally long sections of a fiber identical to the one in the first arm by splicing in between them equally long section of a different fiber with larger attenuation. This way, the number of Cerenkov photons reaching the SiPM at the end of the second arm will be smaller than the number reaching the SiPM in the first arm by a factor depending on how many section of the more attenuating fiber were crossed and, therefore, on the position of the loss.

Simulation studies indicate that this sensor has the ability to achieve a resolution of down to a few centimeters, depending mainly on the length of the spliced fiber sections in the second sensor. In addition, each signal is read independently and the absolute position is then calculated from the intensity ratio in the two branches. This guarantees that there is no overlap of the signals and it becomes possible to detect multiple signals without using clock triggers.

The high spatial resolution of the monitor is particularly relevant when there is the need to monitor losses in narrow spaces as for example in the CLIC Experimental

#Corresponding author : angela.intermite@quasar-group.org

area (CLEX). In this test facility, two beams run parallel to each other: the drive beam and the probe beam.

The accelerator hall of the CLEX building, shown in Fig. 1, measures 42.5 m by 8 m, and the distance between the two beams is about 0.75 m.

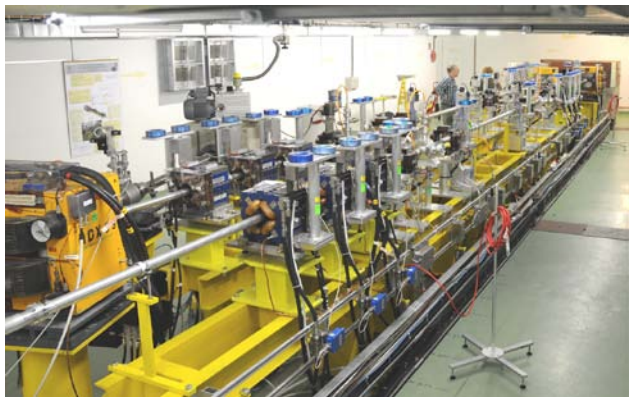

Figure 1: Photo of the CLEX area, showing the two beam pipes running parallel to each other.

This contribution will focus on the characterization of the photon detector used for this project, the SiPM.

## *SiPM Structure and working principle*

A SiPM is composed of an array of Single Photon Avalanche Diode (SPAD) cells, combined to form a macroscopic unit. In most of the SiPMs that have been studied in the frame of this work, about 500 cells are used to cover an area of 1 $mm^2$. Each cell operates in limited Geiger mode, a few Volts above the breakdown voltage. In this working mode, the device can remain in a steady state until a free carrier such as an incident photon enters into the depletion zone. This photon generates an electron/hole pair, acting as a charge carrier that is accelerated by the electric field set by the bias voltage provided, releasing other carriers by impact ionization. Being the bias voltage above breakdown, the liberated carriers acquire enough energy to ionize more carriers in turn, resulting in triggering a self-sustaining avalanche. The avalanche is then quenched by suitable external circuitry, which includes a large load resistance for the current and hence limits the current flow in the detector. Limiting the current flow turns off the avalanche and allows the detector to recover and be able to detect another photon [7, 8].

The general features that are required to ensure detection of most incident photons are:

- Low dark count;
- Low pixel to pixel optical coupling;
- High photo detection probability;
- Fast time response;
- Low after pulsing;

Depending on the device structure, recovery times ranging from 3 ns to 50 ns can be observed. A typical SiPM signal is shown in Fig. 2.

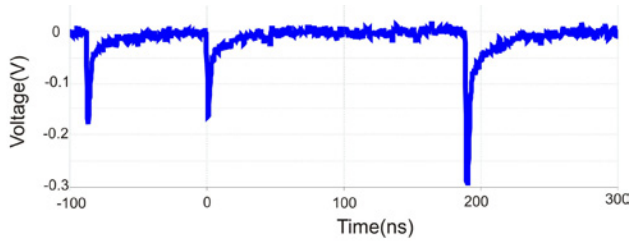


Figure 2: Example of a typical SiPM signal that illustrates the recovery time of a single cell after a signal peak.

## *Dark Noise*

In addition to the real signal, electron/hole pairs can also be generated in the depletion region of a SiPM by thermal generation of carriers through Shockley-Read-Hall (SRH) recombination-generation centers or by bulk diffusion of minority carriers from the quasi-neutral region. The generation of electron/hole pairs and thermal bulk diffusion represents the characteristic noise of this type of detectors and, being undistinguishable from the real signal, sets a limit for the ultimate sensitivity of these devices. In the absence of light, the electrical effect of these mechanisms is referred to as dark count rate and determines the number of noise counts generated in the detector per second.

In a SiPM the instantaneous current that is conserved everywhere in the circuit is given by [9]:

$$i(t) = \frac{A}{V}\sum_{n} - qv_{xn} = -q\frac{N}{L} < v_x >_N$$

Where $A$, $V$ and $L$ refer, respectively, to the area, the volume and the length of the SiPM and the sum over $n$ is performed for all $N$ carriers in the device. $v_x$ is the carrier velocity along the x axis.

The average instantaneous current is zero. However, since the velocity and the number of carriers can fluctuate, $i(t)$ generally is not exactly zero at any given time. This small deviation from zero is responsible for the so-called *current noise*.

Two sources of noise coexist in this last equation for the *current noise*:

- Thermal or Johnson/Nyquist noise: the velocity of each carrier fluctuates due to scattering during thermal motion.
- Generation-recombination noise: the number of carriers fluctuates because of generation-recombination processes.

When it comes to the application, the dark noise influences the performance of the detector depending on the specific light intensity level to be monitored.

When the photon flux is high, provided the detector is not saturated, i.e. when the number of photons per nanosecond is larger than 1 and smaller than about 250 for a 500 cells SiPM, one has a considerable increase in the number of cells firing within the time scale that is typical for the development of the avalanche; 1÷5 ns in optimum operating conditions. This results in an overlap of the signals of different cells, thus producing

proportionally higher signal peaks. This allows to clearly distinguish these events from the peaks caused by noise, which are mainly single cell events, by setting a discrimination threshold. On the other hand, when the photon flux is low enough that the probability of more cells firing in a window of few nanosecond is small (<50 photons per μs), one must resort to count single cell peaks. This makes it difficult to easily discriminate the dark counts from the signal of interest and hence results in an error added to the measurement. Therefore, it sets a limit to the minimum photon rate detectable.

### *Other Sources of Noise*

There are several other sources of noise that can contribute to the total noise in the SiPM signal. Depending on the respective working conditions these can become dominant and should therefore always be carefully considered:

- *Gain noise* is specific to avalanche detectors. All avalanche photodiode generate excess noise due to the statistical nature of the avalanche process. This noise results in varying the amount of charge created in the avalanche from time to time, producing a broadening of the signal peak spectrum. The gain noise factor is a function of the carrier ionization ratio *k*. *k* increases strongly with the electric field across the structure, i.e. with the bias voltage provided, and also depends on the doping profile. In the Geiger mode, where the SiPM is biased above the breakdown voltage for operation at very high gain, this noise becomes particularly relevant, leading to rather broad peaks in the signal spectrum (see Fig.6). It can be reduced by cooling.
- *Cross-talk* due to the migration of photons towards neighboring pixels. Hot carriers in avalanche p-n junction can emit photons even in the visible range, which then fall in the detection range of other pixels. There are 3 different ways of cross talk, differing in the way the created photon reaches the neighboring pixel: direct, inside the depletion layer and through reflection. A solution to avoid the first way of cross-talk is to isolate pixels optically by trenches filled with an opaque material, whilst the others can be reduced by improving the purity of the material used and especially during the manufacturing process, where it is essential to avoid defects. All of this depends on the manufacturer and influences the choice of the supplier. In later sections it will be shown how drastically the cross talk depends indeed on the actual SiPM model tested.
- *After pulsing* caused by trapping centers in the depletion layer. Traps may result from the damage caused by an implantation in the fabrication process of the SiPM. These centers appear as deep levels in the energy gap of the semiconductor. They trap some avalanche carriers and release them with a statistical delay. If the delay is greater than the dead time after the previous avalanche pulse, a released carrier can re-trigger an avalanche and cause a statistically correlated pulse. The probability that an afterpulse occurs increases with the amount of charge that flows through the diode during a Geiger discharge. Thus, the afterpulsing probability increases with the increase of the bias voltage.

## EXPERIMENTAL SETUP

Detailed studies of different SiPMs were carried out in an optical lab at the Cockcroft Institute. The setup illustrated in Fig. 3 was installed inside an optical black box to shield the ambient light.

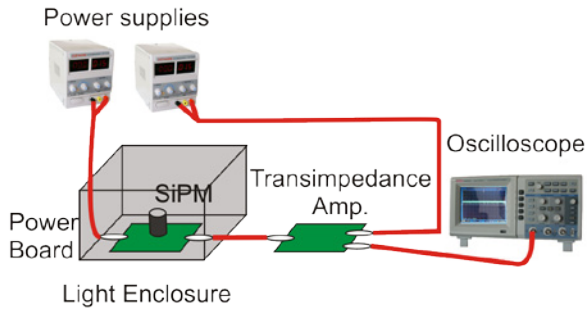


Figure 3: Illustration of the experimental setup used to characterize the SiPM dark noise.

The active surface of every tested SiPM was 1 $mm^2$. The number of cells ranged from 400 to 500 pixels. All models are equipped with an antireflective coating layer on every pixel. In addition, the quasi-neutral region thickness above the thin junction depletion layer is reduced to enhance the spectral response in the blue and near-ultraviolet wavelength ranges. Finally, each elementary cell is surrounded by a suitable trench filled with opaque material to drastically reduce the probability of optical crosstalk between neighbouring cells.

All SiPMs are not cooled and measurements were taken at room temperature.

### *Results*

Tests measurements were done for the SiPMs of three different suppliers (ST-Microelctronics, Photonique, SensL), measuring the dark count rate and the peak height spectrum for each of them as a function of the bias voltage. In addition, 8 prototype detectors, which have yet to be released for commercial use, were tested.

It is important to study the behaviour of the noise when modifying the bias voltage since increasing the bias voltage is the main way to increase the sensitivity of the detector and the signal to noise ratio.

To illustrate this, Fig. 4 indicates the behaviour of a typical signal as a function of the bias voltage for a selection of the samples considered in this study: by increasing the bias voltage, the peak height increases, as it is expected: A higher bias voltage leads to more energetic carriers able to produce more ionizations. The same effect

also influences the dark noise signals, which are also described by plots identical to the one in Fig.4.

Bringing the bias voltage up by 3V produces an increase in the signal by a factor of 3. However, it must be noted that the signal rise time also increases by a similar factor.

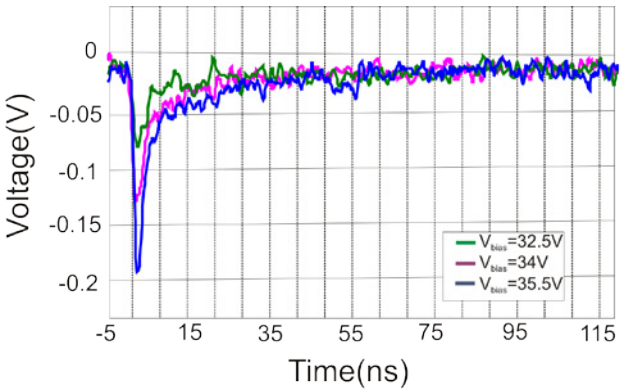


Figure 4: Variation of the dark count signal as a function of the bias voltage.

On the other hand, increasing the bias voltage also increases the probability of thermal generation of electron/hole pairs in the depletion region, resulting in an increase in the overall dark count rate. Fig. 5 shows measurements of the dark count rate for different SiPMs. All models have a breakdown voltage of about 29.5 V. A typical value of dark count rate for these devices is 1 MHz/mm$^2$, measured at a bias voltage of 32 V. Increasing the bias voltage by 3 V also produces an increase of the overall dark count rate of a factor 3.

Since the dark count rate is very high and depends on the temperature as well as on the overvoltage, a possible solution for reducing the noise is using a thermoelectric cooler (TEC) to guarantee temperature stability [10]. On the other hand, the trap lifetime in the depletion layer increases with lower temperatures, resulting in an increased after pulsing.

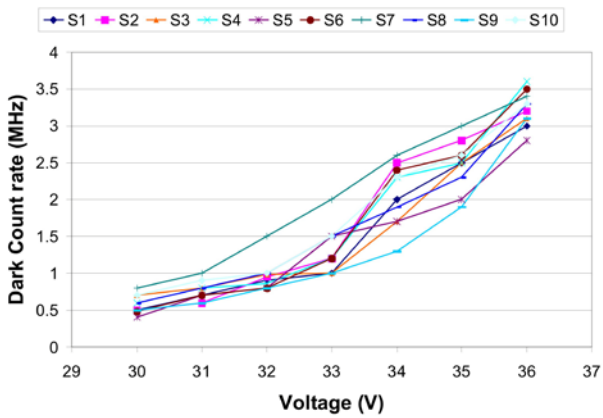


Figure 5: Variation of the dark count rate as a function of the bias voltage for 10 different SiPMs

To assess the contribution of rising the bias voltage on cross-talk noise, a more detailed analysis of the dark noise peak height spectra has been carried out.

If cross-talk was not present at all, the occurrence of double peaks, i.e. when two pixels fire simultaneously, and hence when the SiPM produces a voltage drop twice as high, should be only a statistical effect. This would lead to a spectrum following a Poissonian distribution. Any deviation from this spectral shape, in which higher voltage drops occur more frequently, can be safely attributed to cross-talk contribution to the dark noise.

Figure 6 shows 2 cross-talk spectra corresponding to the same SiPM sample for 2 different bias voltages. It can be seen how the peak amplitude moves rightwards, increasing with increasing bias voltage, in accordance with Fig. 4. The peak height ratio between the first and the second peak also increases by a factor of 1.7 when increasing the bias voltage by 3V, showing how the bias voltage increases the cross-talk effect, even though this contribution to noise is slightly less severe than the one on the overall count rate described in the previous paragraph.

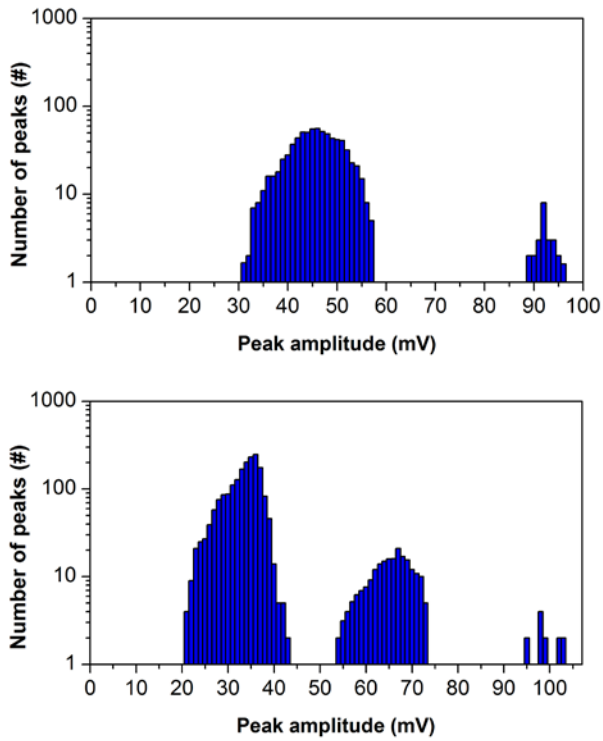


Figure 6: Peak height spectra for the same SiPM sample with two different bias voltages of 29.5V and 32.5V.

Finally, to show the importance of manufacturing techniques on the occurrence of cross-talk, peak height spectra at the same bias voltage of 32V for different SiPM samples were acquired, three examples are shown in Figure 7.

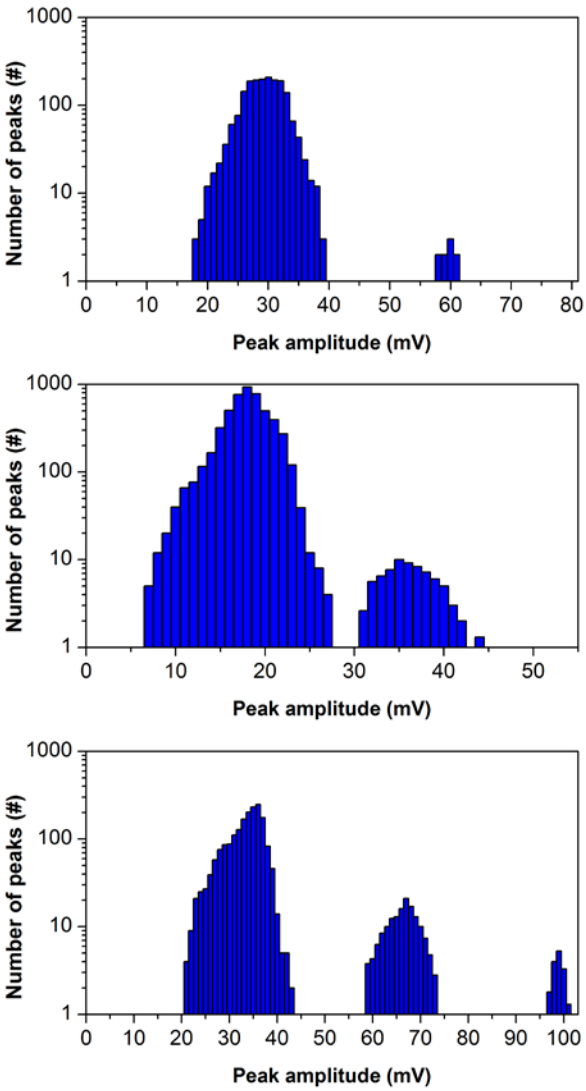


Figure 7: Plots of dark noise spectra at a bias voltage of 32 V for different SiPM samples.

Three different behaviors were observed. In the first and second plot 2 peaks were measured: the highest one, occurring at lower peak amplitude, is due to a single pixel firing, whilst the shortest is due to two different pixels firing in parallel. The last plot shows a different characteristics were even three different pixels were activated in parallel. The height ratio between the first two peaks shows an increasing occurrence of cross-talk in the three samples, differing by a factor of 1.3 between the first and the second sample, and even by a factor of 8 between the first and the third, showing how better manufacturing can improve the cross-talk performance by an order of magnitude.

These measurements allow thus to characterize the quality of different samples in terms of the cross-talk signal.

## CONCLUSION

In this contribution the main sources of dark noise, i.e. the thermal generation of electron-hole pairs in the depletion layer and the optical crosstalk, which limit the performances of SiPM were analyzed and characterized, describing their response to different bias voltages and manufacturing techniques.

Experimental tests on several commercial and pre-release samples yielded a typical dark count rate of about 1 MHz/mm$^2$ for a bias voltage of about 2V above the breakdown value for essentially all samples. Increasing the bias voltage was shown to proportionally increase the signal peak height and overall dark count rate by similar factors of about 3 for a 3V increase, while showing a slighter effect on increasing the cross-talk by a factor of 1.7 for the same voltage increase.

The influence of manufacturing techniques on the cross talk was instead found to be severe, with spectra from different samples showing a difference in cross-talk occurrence by almost an order of magnitude.

Further tests and data acquisition are currently been carried out to improve the characterization of these devices and to select the best commercially available sample for a future beam loss monitor at CTF3/CLIC.

## REFERENCES

[1] N. Nightingale, “A new silicon avalanche photodiode counting detector module for astronomy,” Experimental Astronomy 1, pp. 407-422, 1991.

[2] F. Zappa, G. Ripamonti, A. Lacaita, S.Cova and C. Samori, ”Tracking capabilities of SPADs for laser ranging,” 8th International Workshop on Laser Ranging Instrumentation, Annapolis, MD, USA, pp. 25-30, May 1992.

[3] G. Ripamonti, M. Ghioni and S. Vanoli, “Photon timing OTDR: A multiphoton backscattered pulse approach,” Electronics Letters 26, pp. 1569-1572, December 1990.

[4] F. Wulf, M. Korfer, “Local beam losses and beam profile monitoring with optical fibers,” Proceedings of DIPCA09, Basel, Switzerland.

[5] J. V. Jelley, “Cerenkov Effect and Its Applications”, British J. of Appl. Phys. 6, 1955, p. 227-232.

[6] P. Gorodetsky et al, “Quartz Fiber calorimetry”, Phys. Rev. Lett. 25 (1997), 56.

[7] P. Finocchiaro et al, “Characterization of a Novel 100-Channel Silicon Photomultiplier-Part 1: Noise”, IEEE Trans. On Electron Devices 55 (10), October. 2008, p. 2757 - 2762.80

[8] P. Finocchiaro et al, “Characterization of a Novel 100-Channel Silicon Photomultiplier-Part 2: Charge and Time”, IEEE Trans. On Electron Devices 55 (10), October. 2008, p. 2765 – 2772.

[9] E. Rosencher and B. Vinter, “Optoelectronics,” Cambridge University Press 2002.

[10] P K Lightfoot, G J Barker, K Mavrokoridis, Y A Ramachers and N J C Spooner , “Characterisation of a silicon photomultiplier device for applications in liquid argon based neutrino physics and dark matter searches,” Journal of Instrumentation, Vol. 3, 2008.